Temperature- and Pressure-Induced Phase Transitions in *p*-Difluorobenzene Crystals

Yuji Towata, Yoshio Suzuki,† Yoshinori Nibu, Hiroko Shimada,* and Ryoichi Shimada†

Department of Chemistry, Faculty of Science, Fukuoka University, Nanakuma, Jonan-ku, Fukuoka 814-0180

†Department of Electronics, Faculty of Technology, Fukuoka Institute of Technology,
Wajiro-Higashi, Higashi-ku, Fukuoka 811-0295

(Received February 13, 2001)

The temperature and pressure effects on the Raman-active inter- and intramolecular vibrations of [$^1H_4$]- and [$^2H_4$]*p*-difluorobenzene crystals were studied. The observed spectral structure, and the temperature and pressure dependences on the vibrational frequencies of the inter- and intramolecular vibrations indicate the following facts: (1) The temperature-induced phase transitions take place at about 235 and 195 K under 1 atm in [$^1H_4$]- and [$^2H_4$]*p*-difluorobenzene crystals. (2) The pressure-induced phase transition takes place under about 2.7 and 2.8 GPa at 298 K in [$^1H_4$]- and [$^2H_4$]*p*-difluorobenzene crystals, respectively. (3) A weak C–H···F–C intermolecular interaction exists in crystals.

The Raman spectra of molecular crystals give information for studying the phase transitions in crystals, because the spectral structure and the frequency of the intermolecular vibrations change sensitively with changes in the intermolecular interaction caused by phase transitions. We have discussed the phase transitions and the intermolecular interactions in 1,2,4,5-tetrahalo- and hexahalobenzene crystals based on observations of the temperature and pressure effects on the Raman active inter- and intramolecular vibrations.[1–6] We also carried out calculations of the pressure-induced frequency shifts for the intramolecular vibrations, and showed that the observed pressure dependence on the frequency shift is mainly caused by an intermolecular repulsive force between the halogen atoms belonging to the adjacent molecules in these crystals. Very recently, we studied the pressure effect on the intramolecular vibrations in cyanuric chloride crystal, and showed that the intermolecular donor-acceptor interaction plays an important role for the extensive network structure in the crystal.[7]

Although the intramolecular vibrations of *p*-difluorobenzene have been studied by several workers,[8,9] no studies concerning the intermolecular vibrations have been reported, although the inter- and intramolecular vibrations of *p*-dichloro- and -dibromobenzene crystals have been investigated by many workers.[10–13] The crystal structure of *p*-difluorobenzene was studied by Thalladi et al.[14] and the nature of C–H···F–C intermolecular interactions in the crystal was discussed. They pointed out that the C–F group prefers to form C–H···F–C intermolecular interactions, rather than F···F interactions, in *p*-difluorobenzene crystal, whereas the heavier halogens, such as chlorine and bromine atoms, seem to prefer formation of halogen···halogen interactions in *p*-dichloro- and -dibromobenzene crystals.

This work is intended to study the phase transitions and the existence of C–H···F–C interactions in *p*-difluorobenzene crystals through observations of the temperature and pressure effects on the Raman active inter- and intramolecular vibrations as well as differential scanning calorimetric measurements.

Experimental

Material. [$^1H_4$]- and [$^2H_4$]*p*-difluorobenzenes (*p*FB-d_0 and *p*FB-d_4) were obtained from Wako Chemicals and Aldrich Chemical Co., respectively. *p*FB-d_0 was purified by repeated vacuum distillations and *p*FB-d_4 was used without further purification.

Optical Measurement. The Raman spectra of *p*FB-d_0 and *p*FB-d_4 crystals in the inter- and intramolecular vibrational regions were measured with a JOBIN YVON T64000-FU Laser Raman Spectrophotometer. The spectra were observed at various temperatures between 77 and 250 K under 1 atm and under various pressures from 1 atm to 8 GPa at 298 K by the backscattering observation method. A diamond anvil cell, obtained from Toshiba Tungaloy Co., was used for measurements of the Raman spectra under various high pressures. A cryostat of OXFORD DN1704 was used for measurements of the Raman spectra at various temperatures. The method to observe the Raman spectra was exactly the same as that described previously.[1–5] The temperature of the cryostat was raised from 77 K at a heating rate of about 2 K min^{-1} up to the required temperature, and the observation was made after the temperature was kept at constant for 20 min. Pressure was applied to the anvil cell by about 0.2 GPa and the cell was allowed to stand overnight. The 514.5, 488.0, and 476.5 nm beams from an Spectra Physics Model 2017-04S Ar$^+$ ion laser were used for excitation. Polarization measurements showed that a sample cooled quickly at 77 K gave unpolarized Raman bands. The pressure inside the gasket hole was determined by measuring the wavelength shift of the R_1 fluorescence line at 694.2 nm emitted from the ruby chips according to the equation proposed by Mao et al.[15] The pressure inside the hole was confirmed to be hydrostatic by observing the shapes of the R_1 and R_2 (692.7 nm) fluorescence lines emitted from ruby. A calorimetric experiment was made with a Seiko Denshi Model SSC/5200 Differential Scanning Calorimeter at a heating rate of 5 K min^{-1} in the temperature range between 77 and 250 K under 1 atm.

Results and Discussion

Temperature Effect on Intermolecular Vibrations. The crystal structure of *p*-difluorobenzene belongs to the monoclinic space group $P2_1/c$ with two molecules in the unit cell at 215 K.[14] According to group theory, the six rotational intermolecular vibrations are Raman active in this crystal phase; these vibrations are classified into symmetry species $\mathrm{a_g}$ and $\mathrm{b_g}$, three vibrations belonging to each species.

The Raman spectra observed at 77, 195, and 235 K are shown in Fig. 1. The observed low-frequency Raman spectra of *p*FB-d_0 and *p*FB-d_4 crystals show that (1) the Raman bands become broad and shift wholly to the lower frequency side with increasing temperature, (2) the spectral structure remains unchanged with raising temperature from 77 to 190 K, and the structure changes at around 195 K, and (3) the spectral structure remains unchanged again with raising temperature from 195 to 230 K, and the structure changes at around 235 K. The curves for the temperature dependence on the vibrational frequency (temperature–frequency curves) are given in Fig. 2. The Raman bands observed at 77, 195, and 235 K are called (a, b, c, d, e), (α, β, γ, δ, ε), and (A, C, D, E), respectively, as shown in Fig. 1. The frequencies of these bands are given in Table 1, together with the isotopic factors of the corresponding frequencies ($\tilde{\nu}(p\mathrm{FB}\text{-}d_0)/\tilde{\nu}(p\mathrm{FB}\text{-}d_4)$). The bands at 195 K can be ascribed to the intermolecular vibrations in the phase belonging to the monoclinic space group $P2_1/c$ with two molecules in the unit cell. The observed isotopic factors of the corresponding frequencies were calculated to be 1.02, 1.00, 1.01, 1.11, and 1.11 for bands α, β, γ, δ, and ε, respectively. If the low-frequency Raman bands are ascribable to the rotational intermolecular vibrations, the isotopic factor of the frequencies is related to the isotopic factor of the moments of inertia, given by the relationship $\tilde{\nu}(p\mathrm{FB}\text{-}d_0)/\tilde{\nu}(p\mathrm{FB}\text{-}d_4) = (I_r(p\mathrm{FB}\text{-}d_4)/I_r(p\mathrm{FB}\text{-}d_0))^{1/2}$, where I_r is the moment of inertia of the molecule about the axis $r(= x, y, \text{or } z)$. The x axis is taken perpendicular to the molecular plane, and the y and z axes are in the plane with the z axis passing through two fluorine atoms. The values of the moments of inertia of *p*FB-d_0 and *p*FB-d_4 were calculated using the molecular structures given by Thalladi et al.[14] The values ranged in the order $I_x > I_y > I_z$. The isotopic factors for the moment of inertia, $(I_r(p\mathrm{FB}\text{-}d_4)/I_r(p\mathrm{FB}\text{-}d_0))^{1/2}$, were calculated to be 1.027, 1.008, and 1.098 about the x, y, and z axes, respectively. These values correspond well to the observed values of $\tilde{\nu}(p\mathrm{FB}\text{-}d_0)/\tilde{\nu}(p\mathrm{FB}\text{-}d_4)$, and, therefore, bands α, β, γ, δ, and ε can be ascribed to be due to the rotational intermolecular vibrations about the x, y, y(?), z, and z axes, respectively. The values of $\tilde{\nu}(p\mathrm{FB}\text{-}d_0)/\tilde{\nu}(p\mathrm{FB}\text{-}d_4)$ for bands A, C, D, and E observed at 235 K are 1.02, 1.01, 1.08, and 1.08, respectively, and the values for bands a, b, c, d, and e observed at 77 K are 1.02, 1.00, 1.01, 1.11, and 1.10, respectively. These values correspond well to the calculated $(I_r(p\mathrm{FB}\text{-}d_4)/I_r(p\mathrm{FB}\text{-}d_0))^{1/2}$ values and, therefore, bands A, C, D, and E at 235 K, and bands a, b, c, d, and e at 77 K can all be ascribed to the rotational intermolecular vibrations.

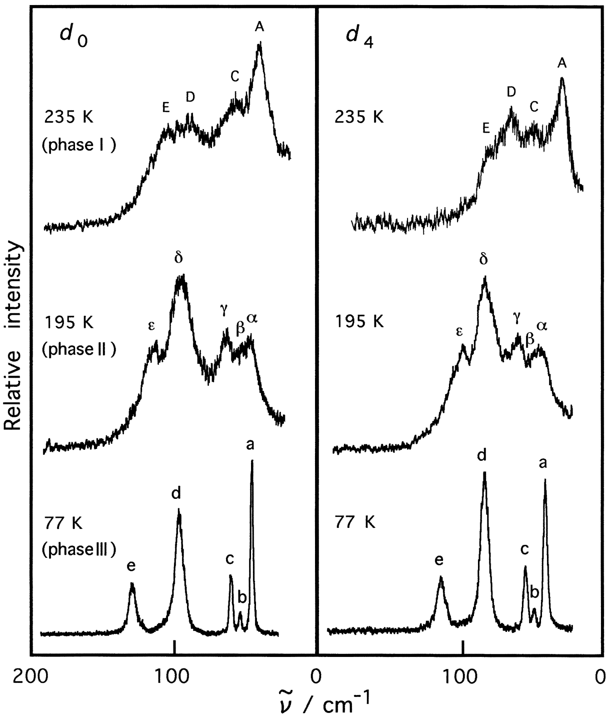

Fig. 1. The Raman spectra of [^{1}H$_4$]- and [^{2}H$_4$]*p*-difluorobenzene crystals in the intermolecular vibrational region observed at various temperatures under 1 atm. d_0 and d_4 refer to [^{1}H$_4$]- and [^{2}H$_4$]*p*-difluorobenzene crystals, respectively.

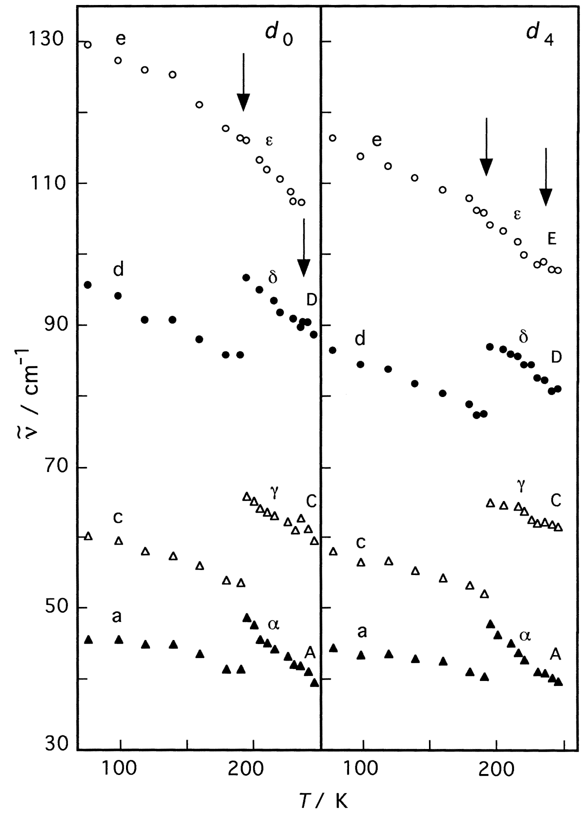

Fig. 2. Temperature-frequency curves for [^{1}H$_4$]- and [^{2}H$_4$]*p*-difluorobenzene crystals in the intermolecular vibrational region observed at various temperatures under 1 atm.

Table 1. Raman Frequencies due to Intermolecular Vibrations of [$^1H_4$]- and [$^2H_4$]*p*-Difluorobenzene Crystals at Various Temperatures under 1 atm

[$^1H_4$]*p*-Difluorobenzene

	235 k				195 k					77 k				
band	A	C	D	E	α	β	γ	δ	ε	a	b	c	d	e
$\tilde{\nu}$/cm^{-1}	42	63	90	107	49	56	66	97	116	45	53	60	96	128

[$^2H_4$]*p*-Difluorobenzene

	235 k				195 k					77 k				
band	A	C	D	E	α	β	γ	δ	ε	a	b	c	d	e
$\tilde{\nu}$/cm^{-1}	41	62	83	99	48	56	65	87	104	44	53	59	86	116
I. F.[a)]	1.02	1.01	1.08	1.08	1.02	1.00	1.01	1.11	1.11	1.02	1.00	1.01	1.11	1.10
Assign[b)]	R_x	R_y?	R_z	R_z	R_x	R_y	R_y?	R_z	R_z	R_x	R_y	R_y?	R_z	R_z

a) Isotopic factor of frequency, $\tilde{\nu}$(*p*FB-d_0)/$\tilde{\nu}$(*p*FB-d_4).

b) R_x, R_y, and R_z refer to the rotational intermolecular vibrations about *x*, *y*, and *z* axes, respectively.

The temperature–frequency curves given in Fig. 2 show that discontinuous points are detected at about 195 and 235 K. The changes in the spectral structure and the discontinuous frequency shifts in the temperature–frequency curves suggest that the intermolecular interaction in *p*FB-d_0 and *p*FB-d_4 crystals changes as the temperature decreases and the phase transitions take place at temperatures of around 235 and 195 K under 1 atm. The phases of the crystal are called phases I, II, and III with decreasing temperature from 245 K. The discontinuity is more distinctly detected at 195 K than at 235 K. This observation indicates that the intermolecular interaction greatly changes for the phase transition from II to III than that from I to II. The facts that the five Raman bands were observed and the observed isotopic factors of the frequencies in phases I and III correspond well to the rotational intermolecular vibrations may suggest that the structures of *p*FB-d_0 and *p*FB-d_4 crystals in phases I and III belong to one of the space groups with symmetry C_{2h} belonging to a base-centered lattice with two molecules in the unit cell.

Pressure Effects on Intermolecular Vibrations. The Raman spectra of *p*FB-d_0 and *p*FB-d_4 crystals observed in the intermolecular vibrational region under various pressures at 298 K are shown in Fig. 3. The pressure–frequency curves are given in Fig. 4. The frequencies of these bands are given in Table 2, together with the isotopic factors of the corresponding frequencies, ($\tilde{\nu}$(*p*FB-d_0)/$\tilde{\nu}$(*p*FB-d_4)). The spectra observed under 1.1(0.9) GPa consist of five bands (ζ, α, γ, δ, ε), and the structure is the same as that observed at 195 K shown in Fig. 1, except for band ζ (in Fig. 3) being not clearly detected in the spectra shown in Fig. 1. The pressures written outside and inside the parentheses correspond to those applied to *p*FB-d_0 and *p*FB-d_4 crystals, respectively. From this fact, the spectra observed under 1.1(0.9) GPa could be ascribed to the spectra due to phase II. Bands α, γ, δ, and ε can be assigned to the rotational intermolecular vibrations about the *x*, *y*(?), *z*, and *z* axes, respectively, from a comparison with the band structure of the spectra due to phase II shown in Fig. 1, and from the isotopic factor of the frequency. Band ζ could be ascribed to the rotational intermolecular vibration about the *x* axis from the values of the observed frequencies under 1.1(0.9) GPa. The spectral structure changes with successive applications of pressure. The spectra observed under 3.7(4.0) GPa consist of six bands (1, 2, 3, 4, 5, 6), and are different from the spectra observed under 1.1(0.9) GPa and also from the spectra due to phase III shown in Fig. 1. Therefore, the spectra observed under 3.7(4.0) GPa could be ascribed to the spectra due to another phase, which is called phase IV. The spectra observed under 3.0(3.3) GPa can be explained by an overlapping of the bands due to phases II and IV, suggesting that the crystal under about 3 GPa may coexist in phases II and IV. The coexistence of the crystal in phases II and IV can be well seen in Fig. 4. A discontinuous frequency shift was detected under about 2.7 and 2.8 GPa in *p*FB-d_0 and *p*FB-d_4 crystals, respectively. The discontinuous point in the curves shown in Fig. 4 and the change in the spectral structure shown in Fig. 3 indicate that the phase transition from phases II to IV takes place under about 2.7 and

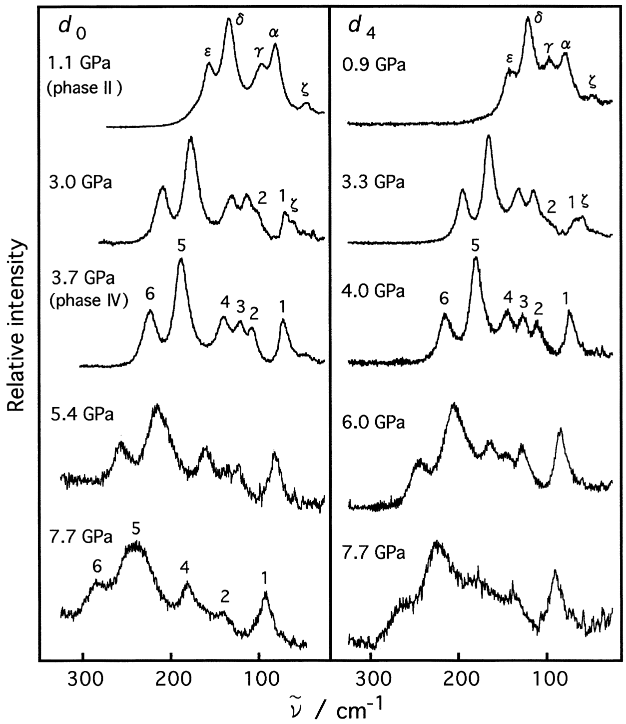

Fig. 3. The Raman spectra of [$^1H_4$]- and [$^2H_4$]*p*-difluorobenzene crystals in the intermolecular vibrational region observed under various pressures at 298 K.

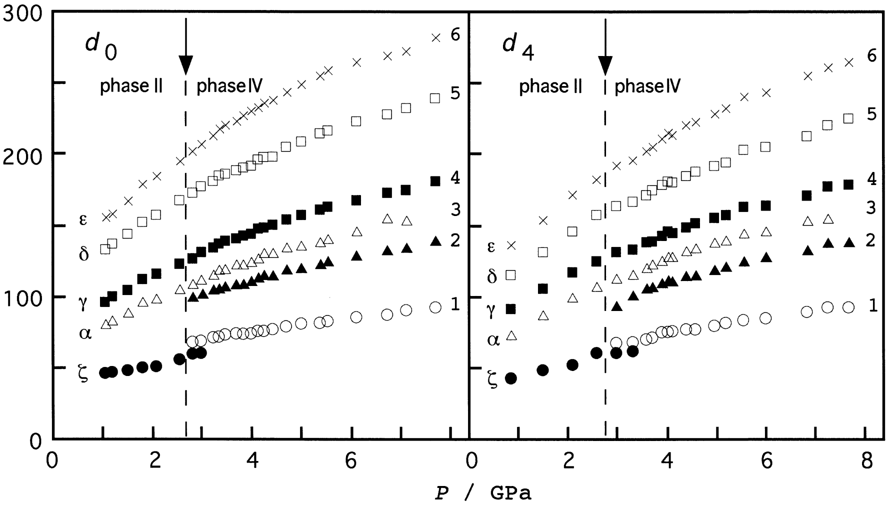

Fig. 4. Pressure–frequency curves for the Raman bands of $[^1\mathrm{H}_4]$- and $[^2\mathrm{H}_4]$*p*-difluorobenzene crystals in the intermolecular vibrational region observed under various pressures at 298 K.

Table 2. Raman Frequencies due to Intermolecular Vibrations of $[^1\mathrm{H}_4]$- and $[^2\mathrm{H}_4]$*p*-Difluorobenzene Crystals under Various Pressures at 298 k

$[^1\mathrm{H}_4]$*p*-Difluorobenzene

	1.1 GPa					3.5 GPa						7.7 GPa				
band	ζ	α	γ	δ	ε	1	2	3	4	5	6	1	2	4	5	6
$\tilde{\nu}$/cm^{-1}	46	81	96	134	156	73	107	120	139	186	222	92	140	181	240	283

$[^2\mathrm{H}_4]$*p*-Difluorobenzene

	0.9 GPa					3.5 GPa						7.7 GPa				
band	ζ	α	γ	δ	ε	1	2	3	4	5	6	1	2	4	5	6
$\tilde{\nu}$/cm^{-1}	43	74	91	115	137	70	106	120	138	172	203	92	139	179	226	266
I. F.[a)]						1.04	1.01	1.00	1.01	1.08	1.09	1.00	1.01	1.01	1.06	1.06
Assign	R_x	R_x	R_y?	R_z	R_z	R_x	R_x?	R_y	R_y?	R_z	R_z	R_x	R_x?	R_y?	R_z	R_z

a) Isotopic factor of frequency, $\tilde{\nu}$(*p*FB-d_0)/$\tilde{\nu}$(*p*FB-d_4).

b) R_x, R_y, and R_z refer to the rotational intermolecular vibrations about *x*, *y*, and *z* axes, respectively.

2.8 GPa in *p*FB-d_0 and *p*FB-d_4 crystals, respectively. The spectral structures remain unchanged from 3.7(4.0) GPa to 7.7(7.7) GPa with increasing pressure, except for band 3, whose intensity decreases with increasing pressure. The observed Raman frequencies under 1.1(0.9), 3.5(3.5), and 7.7(7.7) GPa and the isotopic factors for each bands are given in Table 2. Possible assignments of the observed bands are also given in Table 2.

Temperature Effect on Intramolecular Vibrations. The Raman spectra of *p*FB-d_0 and *p*FB-d_4 crystals observed at 77, 195, and 235 K in the intramolecular vibrational region are given in Fig. 5, and the temperature–frequency curves are shown in Fig. 6. Assignments for some fundamental vibrations are given in Fig. 5 and Table 3. The assignments made in this work are the same as those given by Zimmerman and Dunn,[8] and the nomenclature of the vibrational modes is taken from that given by Mair and Hornig.[16]

Discontinuous points were observed at 195 and 235 K in the temperature–frequency curves given in Fig. 6, and the amount of discontinuity observed at 195 K is larger than that at 235 K. These behaviors are quite similar to those observed for the in-

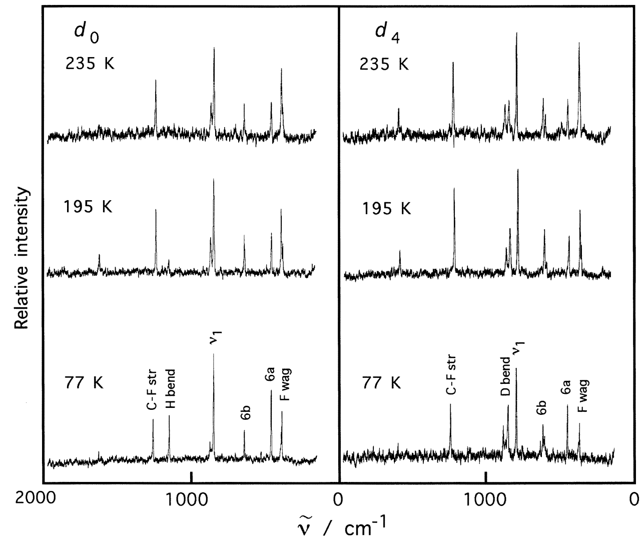

Fig. 5. The Raman spectra of $[^1\mathrm{H}_4]$- and $[^2\mathrm{H}_4]$*p*-difluorobenzene crystals in the intramolecular vibrational region observed at various temperatures under 1 atm.

Table 3. Raman Frequencies due to Intramolecular Vibrations of [$^1H_4$]- and [$^2H_4$]p-Difluorobenzene Crystals at Various Temperatures under 1 atm

		[$^1H_4$]p-Difluorobenzene					[$^2H_4$]p-Difluorobenzene				
		This work				Ref[a)]	This work				Ref[a)]
		245 K	230 K	190 K	77 K	vapor	245 K	230 K	190 K	77 K	vapor
Sym	Mode	$\tilde{\nu}$/cm^{-1}	$\tilde{\nu}$/cm^{-1}	$\tilde{\nu}$/cm^{-1}	$\tilde{\nu}$/cm^{-1}	$\tilde{\nu}$/cm^{-1}	$\tilde{\nu}$/cm^{-1}	$\tilde{\nu}$/cm^{-1}	$\tilde{\nu}$/cm^{-1}	$\tilde{\nu}$/cm^{-1}	$\tilde{\nu}$/cm^{-1}
a_g	ν_2(C–H str)[b)]	3090	3090	3086	3086	3088	2308	2308	2306	2306	2306
	C–F str	1235	1233	1249	1252	1257	1222	1221	1232	1238	1248
	H bend[b)]	1149	1147	1140	1144	1140	845	844	846	851	839
	ν_1	840	840	839	844	859	793	794	791	794	793
b_{2g}	F wag	381	381	376	380	374	372	371	364	369	358

a) Taken from Ref. 8.

b) H is replaced by D in [$^2H_4$]p-difluorobenzene.

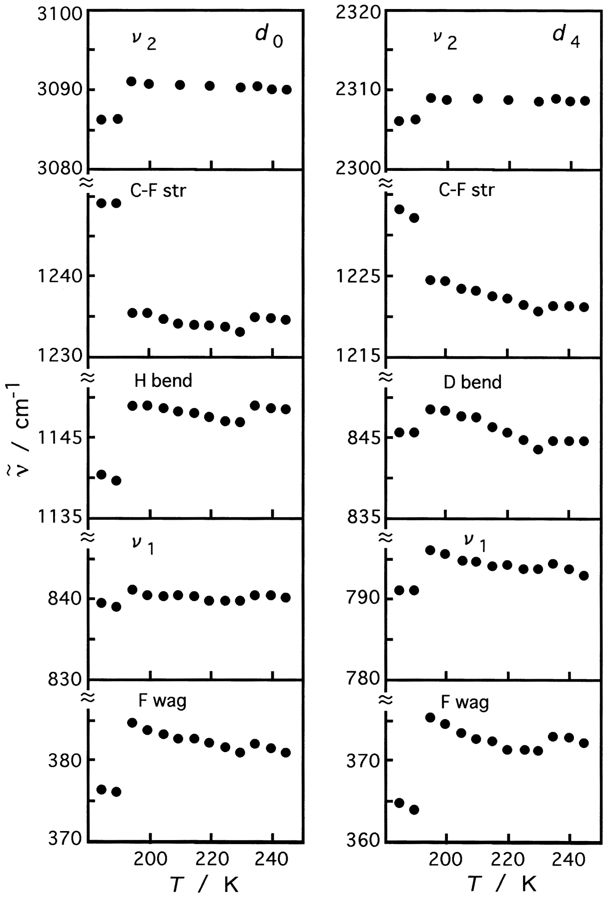

Fig. 6. Temperature-frequency curves for [$^1H_4$]- and [$^2H_4$]p-difluorobenzene crystals in the intramolecular vibrational region observed at various temperatures under 1 atm.

termolecular vibrations. These results suggest that the phase transitions take place at about 195 and 235 K and that the change in the intermolecular interaction due to the phase transition from II to III is much larger than that from I to II.

The two factors are taken into account in a discussion of the frequency shift of the intramolecular vibrations induced by the intermolecular forces in molecular crystals. The first factor is that the intermolecular repulsive and dispersive forces induce large blue and small red shifts, respectively, and, therefore, the frequency of the intramolecular vibrations in molecular crystals increases with increasing intermolecular interactions for all vibrations. When a phase transition takes place in molecular crystals, a discontinuous frequency decrease of the intramolecular vibrations occurs, since the large intermolecular repulsive forces are relaxed by a phase transition.[1–7] The second factor is that the intermolecular donor and acceptor attractive forces resulting from charge transfer give various effects for the frequency shifts of the intramolecular vibrations, that is, the red shift for the frequencies of the correlated stretching vibrations, and the blue shift for the correlated bending and wagging vibrations.

The following facts are derived from Fig. 6 and Table 3: (1) The vibrational frequency of the C–F stretching vibration decreases, while the frequencies of the H(D) bending and F wagging vibrations increase by the change from vapor to phase I in both pFB-d_0 and pFB-d_4. (2) The vibrational frequencies of the C–F stretching, H(D) bending, and F wagging vibrations decrease at 235 K, where the transition from I to II takes place in both pFB-d_0 and pFB-d_4. (3) The frequency of the C–F stretching vibration increases, while the frequencies of the H(D) bending and F wagging vibrations decrease by the transition from phase II to III at 195 K in both pFB-d_0 and pFB-d_4. (4) As for the ν_1 vibration, the vibrational frequency decreases by the change from vapor to phase I in pFB-d_0, while it hardly changes in pFB-d_4. The frequency decreases at 235 and 195 K in both pFB-d_0 and pFB-d_4. (5) As for the C–H stretching vibration, the vibrational frequency hardly changes due to a change from vapor to phase I, and also by transition from I to II, but the frequency decreases at 195 K in both pFB-d_0 and pFB-d_4.

The observed facts (1), (2), and (3) suggest that the intermolecular C–H···F–C donor and acceptor attractive forces act on crystal phases I and II, although the intermolecular donor and acceptor attractive forces hardly act on crystal phase III. The phase transition from II to III causes a relaxation of the intermolecular repulsive forces, and also causes a decrease in the intermolecular C–H···F–C donor and acceptor attractive forces. Discontinuous increases in the frequency of the C–F stretching vibration in phase III are caused by the superiority of the blue shift due to a decrease in the intermolecular C–H···F–C donor and acceptor attractive forces to the red shift, caused by relaxation of the intermolecular repulsive interaction due to phase transition from II to III.

The discontinuous decrease in the frequencies of the H

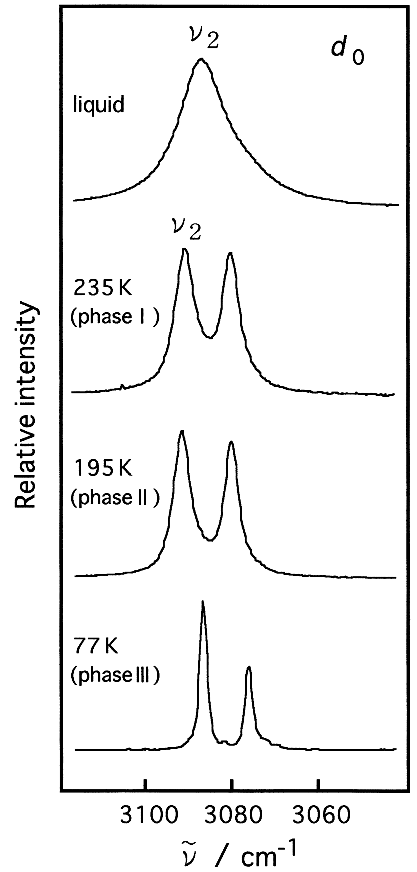

Fig. 7. The Raman band of ν_2 vibration of [$^1H_4$]*p*-difluorobenzene in liquid and crystal phases under 1 atm.

bending and F wagging vibrations in phase III is caused by two factors: a decrease in the intermolecular C–H···F–C attractive forces in phase III and relaxation of the intermolecular repulsive interaction due to phase transition from II to III.

As for the observed fact (4), the decrease in the frequency of the ν_1 vibration of *p*FB-d_0 due to a change from vapor to phase I is attributed to the Fermi-resonance with the $2\nu_{16a}$ mode, while the ν_1 mode of *p*FB-d_4 in phase I is free from the Fermi-resonance.[8] Therefore, the frequency of the ν_1 mode would be hardly affected by the intermolecular donor-acceptor forces. Observed fact (5) is explained as follows. The frequency of the ν_2 vibration should decrease owing to the C–H···F–C intermolecular forces caused by the change from vapor to phase I. The Raman band of the ν_2 vibration of *p*FB-d_0 observed in liquid and vapor splits into a doublet in the crystal phase due to the Fermi-resonance, as can be seen in Fig. 7 and Ref. 8. A splitting of the ν_2 vibration in the crystal phases was also observed for *p*FB-d_4. The competition of the Fermi-resonance and the C–H···F–C intermolecular forces in phase I affects the behavior of the frequency shift of the ν_2 vibration caused by a change from vapor to phase I. The three factors, the Fermi-resonance, the C–H···F–C intermolecular forces, and the relaxation of the intermolecular repulsive interaction due to phase transition, are complicatedly entangled for the frequency change of the ν_2 vibration in phases I, II, and III. The red shift induced by transition from I to II observed for all vibrations is due to relaxation of the intermolecular repulsive interaction due to phase transition from I to II, and this suggests that the intermolecular C–H···F–C donor and acceptor forces still exist in phase II.

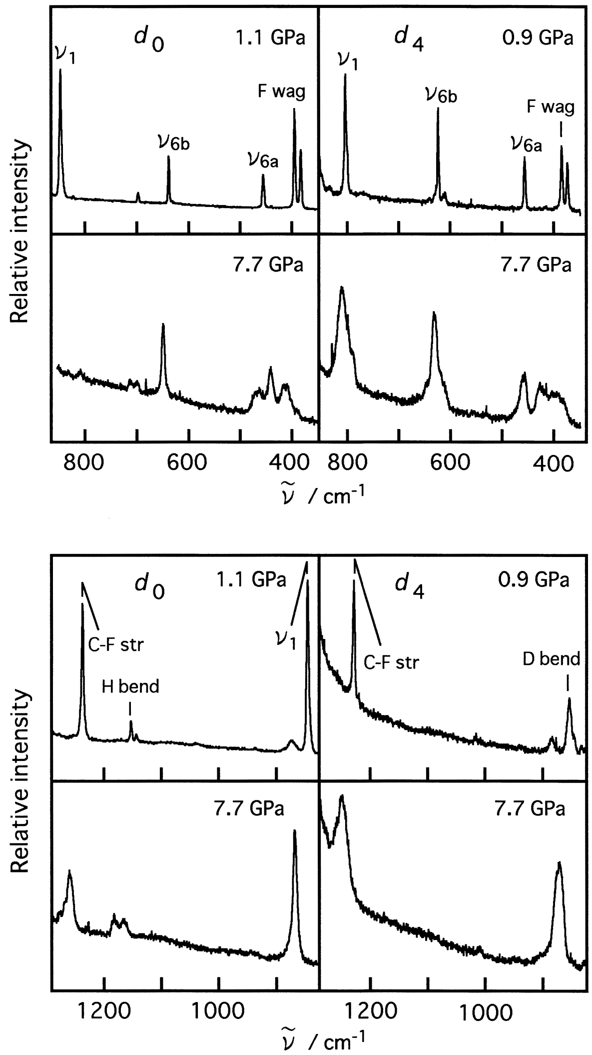

Fig. 8. The Raman spectra of [$^1H_4$]- and [$^2H_4$]*p*-difluorobenzene crystals in the intramolecular vibrational region observed under various pressures at 298 K.

Pressure Effect on Intramolecular Vibrations. The Raman spectra observed under 1.1(0.9) and 7.7(7.7) GPa are shown in Fig. 8 and the observed frequencies of the Raman bands are given in Table 4, together with the assignments. The observed spectral structure in phases IV is essentially the same as that observed in phase II, except for the intensity relationship among the bands, such as the bands due to the ν_{6b} and F wagging vibrations. The pressure-frequency curves are given in Fig. 9. As can be seen in Fig. 9, no discontinuous change in the pressure–frequency curves could be clearly detected under 2.7(2.8) GPa, where the phase transition takes place from II to IV. The bandwidths plotted against pressure (pressure–bandwidth curve) for the ν_2 and ν_{8a} bands for *p*FB-d_0 and *p*FB-d_4 are shown in Fig. 10. The reason why the ν_2 and ν_{8a} bands were selected to discuss the pressure–bandwidth curve is as follows: the Raman bands except for the ν_2 and ν_{8a} bands come to overlap with other bands with increasing pressure and, thus,

Table 4. Raman Frequencies due to Intramolecular Vibrations of [^{1}H$_4$]- and [^{2}H$_4$]*p*-Difluorobenzene Crystals under Various Pressures at 298 K

		[^{1}H$_4$]*p*-Difluorobenzene			[^{2}H$_4$]*p*-Difluorobenzene		
Gpa Sym	Mode	1.1 GPa $\tilde{\nu}$/cm^{-1}	3.5 GPa $\tilde{\nu}$/cm^{-1}	7.7 GPa $\tilde{\nu}$/cm^{-1}	0.9 GPa $\tilde{\nu}$/cm^{-1}	3.5 GPa $\tilde{\nu}$/cm^{-1}	7.7 GPa $\tilde{\nu}$/cm^{-1}
a$_g$	ν_2(C–H str)$^{a)}$	3093	3116	3156	2318	2343	2370
	C–F str	1236	1245	1258	1223	1233	1251
	H bend$^{a)}$	1152	1158	1167	849	857	874
	ν_1	846	855	868	797	802	809
b$_{2g}$	F wag	395	413	441	380	400	428

a) H is replaced by D in [^{2}H$_4$]*p*-difluorobenzene.

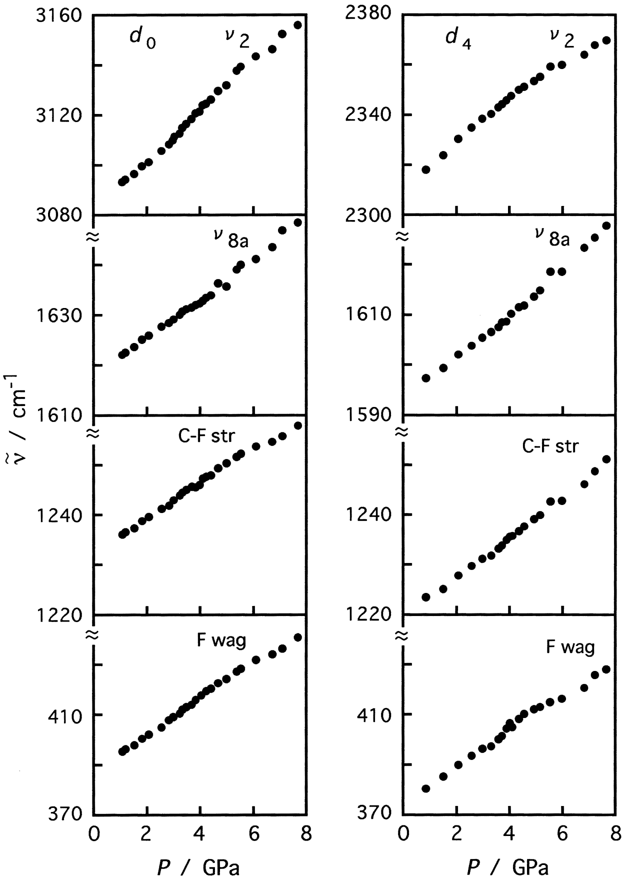

Fig. 9. Pressure–frequency curves for the Raman bands of [^{1}H$_4$]- and [^{2}H$_4$]*p*-difluorobenzene crystals in the intramolecular vibrational region observed under various pressures at 298 K.

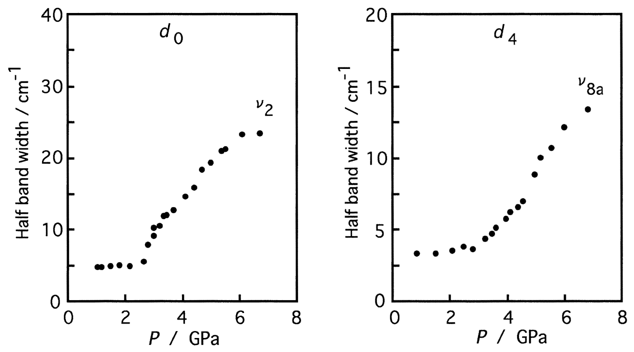

Fig. 10. Pressure–band width curves for the ν_2 and ν_{8a} vibrational bands of [^{1}H$_4$]- and [^{2}H$_4$]*p*-difluorobenzene crystals, respectively.

the bandwidth could be analyzed with high accuracy only for the ν_2 and ν_{8a} bands. A clear discontinuous change was detected under 2.7(2.8) GPa in the pressure–bandwidth curves. This discontinuity indicates that the intermolecular relaxation processes change under 2.7(2.8) GPa and supports the idea that the phase transition from II to IV takes place under 2.7(2.8) GPa in *p*FB-d_0 and *p*FB-d_4 crystals.

The influence of the intermolecular C–H···F–C interaction on the frequency of the intramolecular vibrations was clearly detected in phase II; that is, the frequency of the C–F stretching vibration in phase II is smaller than that in vapor, while the frequency of the F wagging vibration in phase II is larger than that in vapor. The clear discontinuous change in the frequencies of the C–F stretching and F wagging vibrations was not detected under 2.7(2.8) GPa, where the phase transition from II to IV takes place, although a clear discontinuous change was detected at 195 K, where the phase transition from II to III takes place, as described above. This fact may indicate that the intermolecular C–H···F–C interaction still exists in phase IV.

The frequency shift of the intramolecular vibrations induced by intermolecular interactions with the eight neighboring molecules was calculated with changing the intermolecular distance, which was converted into pressure in exactly the same way as described previously.[1–8] The frequency shift of the intramolecular vibrations induced by the intermolecular interaction with other molecules were calculated by[1–8]

$$\Delta\tilde{\nu}_{\text{shift}} = \frac{1}{8\pi^2 c^2 \tilde{\nu}_{Q_n}} \sum_i \sum_j \left(\frac{\partial^2 V_{ij}}{\partial {r_{ij}}^2}\right)\left(\frac{\partial r_{ij}}{\partial Q_n}\right)^2,$$

where Q_n and $\tilde{\nu}_{Q_n}$ are the n-th normal coordinate and its unperturbed vibrational frequency, respectively, r_{ij} is the interatomic distance between atoms i and j belonging to different molecules, and V_{ij} is the potential energy of the atom–atom type due to the intermolecular interaction between two molecules. For the potential V_{ij},

$$2V_{ij} = [-A{r_{ij}}^{-6} + B\exp(-Cr_{ij})]. \tag{1}$$

was used, where A, B, and C are parameters. The values of the

Table 5. Calculated and Observed Pressure-Induced Frequency Shifts for Intramolecular Vibrations of [$^1H_4$]*p*-Difluorobenzene

Mode	Calculated Frequency Shift						Frequency Shift	
	$\tilde{\nu}$1 atm			$\tilde{\nu}_{2.0Gpa}$			$\tilde{\nu}_{2.0Gpa} - \tilde{\nu}_{1\ atm}$ a)	
	Repul $\tilde{\nu}$/cm^{-1}	Disp $\tilde{\nu}$/cm^{-1}	Total $\tilde{\nu}$/cm^{-1}	Repul $\tilde{\nu}$/cm^{-1}	Disp $\tilde{\nu}$/cm^{-1}	Total $\tilde{\nu}$/cm^{-1}	Calcd $\tilde{\nu}$/cm^{-1}	Obsd $\tilde{\nu}$/cm^{-1}
ν_2 (a_g)	16	−3	13	50	−7	43	30	11
C–F str (a_g)	10	−3	7	31	−6	25	18	9
H bend (a_g)	2	−1	1	7	−2	5	4	6
ν_1 (a_g)	7	−2	5	22	−5	17	12	10
F wag (b_{2g})	20	−6	14	43	−11	32	18	22

a) Vibrational frequencies observed at 230 K under 1 atm was taken for the frequencies under 1 atm.

parameters were taken from those given by Spackman.[17] The first and second terms in Eq. 1 represent the dispersive and repulsive energies, respectively. Because the compressibility of *p*-difluorobenzene crystal was not available, the compressibility was assumed to be the same as that of *p*-dichlorobenzene crystal.[18] The calculated pressure-induced frequency shifts, $\Delta\tilde{\nu} = \tilde{\nu}_{2\ \mathrm{GPa}} - \tilde{\nu}_{1\ \mathrm{atm}}$, in phase II are given in Table 5. The vibrational frequency observed at 230 K under 1 atm was used for the frequency under 1 atm.

The facts that (1) the calculated frequency shifts for the C–H and C–F stretching vibrations are larger than the observed shifts and (2) the calculated frequency shifts for the H bending and F wagging vibrations are smaller than the observed shifts support the existence of the intermolecular C–H···F–C donor and acceptor interactions in phase II, since the intermolecular C–H···F–C donor and acceptor interactions were not taken into account in this calculation, which cause the red shift for the stretching vibrations and the blue shift for the bending and wagging vibrations.

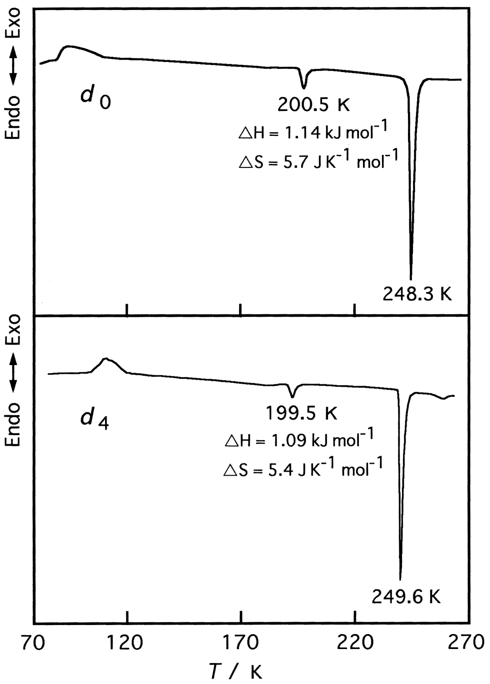

Fig. 11. DSC curves of [$^1H_4$]- and [$^2H_4$]*p*-difluorobenzene crystals measured at temperatures between 77 and 260 K.

Differential-Scanning Calorimetric Measurement. The curves obtained by the differential scanning calorimetric measurement (DSC curve) made for *p*FB-d_0 and *p*FB-d_4 crystals are shown in Fig. 11. A small endothermic peak was observed in addition to the large endothermic peak ascribed to melting of *p*FB-d_0 and *p*FB-d_4 crystals. The temperatures for the small endothermic peaks observed at 200.5 and 199.5 K for *p*FB-d_0 and *p*FB-d_4 crystals, respectively, correspond to the temperatures for the discontinuous change of the frequency of the inter- and intramolecular vibrations in the temperature–frequency curves. Thus, the calorimetric study supports well the result that the phase transition from III to II takes place at around 200 K in *p*FB-d_0 and *p*FB-d_4 crystals. The thermodynamic data, enthalpy change (Δ*H*) and entropy change (Δ*S*) associated with the phase transitions in *p*FB-d_0 and *p*FB-d_4 crystal, obtained by the DSC measurements, are given in Fig. 11. The endothermic peak due to the phase transition from II to I was not detected. This fact may correspond to the observation that the discontinuity in the temperature-frequency curves due to the phase transition from I to II for the inter- and intramolecular vibrations is small compared with the discontinuity due to the transition from II to III. It is expected that the intermolecular interaction forces are not very different from each other in phases I and II.

The studies made on the temperature and pressure effects on the inter- and intramolecular vibrations as well as the DSC measurement lead to the following conclusions: (1) The temperature-induced phase transitions from phases I to II and from II to III take place in the *p*FB-d_0 and *p*FB-d_4 crystals at 235 and 195 K under 1 atm, respectively. (2) The pressure-induced phase transition from II to IV takes place in the *p*FB-d_0 and *p*FB-d_4 crystals under pressures of 2.7 and 2.8 GPa at 298 K, respectively. (3) The C–H···C–F intermolecular donor–acceptor interactions exist in crystal phases I and II.

The authors thank the Japan Private School Promotion Foundation for Science Research Promotion Fund.

References

1 H. Mizobe, H. Shimada, and R. Shimada, *Int. J. Quan. Chem.*, **72**, 287 (1999).

2 S. Matsukuma, H. Kawano, Y. Nibu, H. Shimada, and R. Shimada, *Bull. Chem. Soc. Jpn.*, **67**, 1588 (1994).

3 F. Shimizu, Y. Suzuki, K. Mitarai, M. Fujino, H. Kawano,

Y. Nibu, H. Shimada, and R. Shimada, *Bull. Chem. Soc. Jpn.*, **68**, 1883 (1995).

4 Y. Suzuki, H. Shimada, and R. Shimada, *Bull. Chem. Soc. Jpn.*, **69**, 3081 (1996).

5 G. Sadakuni, M. Maehara, H. Kawano, Y. Nibu, H. Shimada, and R. Shimada, *Bull. Chem. Soc. Jpn.*, **67**, 1593 (1994).

6 Y. Suzuki, R. Shimada, and H. Shimada, *Res. Bull. Fukuoka Inst. Tech.*, **28**, 31 (1995).

7 M. Tanaka, C. Kariu, Y. Suzuki, Y. Nibu, R. Shimada, and H. Shimada, *Bull. Chem. Soc. Jpn.*, submitted.

8 R. L. Zimmerman and T. M. Dunn, *J. Mol. Spectrosc.*, **110**, 312 (1985).

9 A. E. W. Knight and S. H. Kable, *J. Chem. Phys.*, 89, 7139 (1988).

10 S. R. Singh, I. S. Singh, and B. B. Lal, *J. Sci. Res. Banaras Hindu Univ.*, **33**, 91 (1982).

11 S. R. Singh, I. S. Singh, and J. Shamir, *J. Sci. Res. Banaras Hindu Univ.*, **30**, 41 (1979).

12 K. M. M. Kruse, *Spectrochim. Acta*, **26A**, 1603 (1970).

13 H. Shimada, S. Matsukuma, K. Eto, Y. Nibu, and R. Shimada, *Fukuoka Univ. Sci. Rept.*, **23**, 59 (1993).

14 V. R. Thalladi, H. C. Weiss, D. Bläser, R. Boese, A. Nangia, and G. R. Desiraju, *J. Am. Chem. Soc.*, **120**, 8702 (1998).

15 H. K. Mao, P. M. Bell, J. W. Shaner, and D. J. Steinberg, *J. Appl. Phys.*, **49**, 3276 (1978).

16 R. D. Mair and D. F. Hornig, *J. Chem. Phys.*, **17**, 1236 (1949).

17 M. A. Spackman, *J. Chem. Phys.*, **85**, 6579 (1986).

18 S. N. Vaidya and G. C. Kennedy, *J. Chem. Phys.*, **55**, 987 (1971).